The Sensitivity of the Numerical Simulation of the Southwest Monsoon Boundary Layer to the Choice of PBL Turbulence Parameterization in MM5

DAVID R. BRIGHT

NOAA/NWS Weather Forecast Office, Tucson, Arizona

STEVEN L. MULLEN

Department of Atmospheric Sciences, The University of Arizona, Tucson, Arizona

(Manuscript received 19 April 2001, in final form 4 September 2001)

ABSTRACT

Summertime convection over Arizona typically begins in the early afternoon and continues into the night. This suggests that the evolution of the daytime planetary boundary layer is important to the development of Arizona convection. If numerical models are to provide useful guidance for forecasting convection during the monsoon, then the planetary boundary layer must be simulated as accurately as possible through utilization of the appropriate physical parameterizations. This study examines the most appropriate Pennsylvania State University–National Center for Atmospheric Research fifth-generation Mesoscale Model (MM5) planetary boundary layer parameterization(s) for deterministic and ensemble modeling of the monsoon. The four MM5 planetary boundary layer parameterizations tested are the Blackadar, Burk–Thompson, Eta, and medium-range forecast (MRF) schemes. The Blackadar and MRF planetary boundary layer schemes correctly predict the development of the deep, monsoon planetary boundary layer, and consequently do a better job of predicting the convective available potential energy and downdraft convective available potential energy, but not the convective inhibition. Because the convective inhibition is not accurately predicted, it is possible that the MM5's ability to initiate or ''trigger'' convection might be a limiting factor in the model's ability to produce accurate quantitative precipitation forecasts during the monsoon. Since the MM5 planetary boundary layer predicted by the Burk–Thompson and Eta schemes does not accurately reproduce the basic structure of the monsoon planetary boundary layer, their inclusion in a mixed physics ensemble is discussed.

1. Introduction

Forecasting precipitation in the southwest United States during the summer convective season [also known as the North American monsoon, the southwest United States monsoon, the Mexican monsoon, or the Arizona monsoon (Adams and Comrie 1997) and hereafter referred to as the monsoon] is difficult. Observational studies, many motivated by the Southwest Area Monsoon Project (SWAMP; Meitin et al. 1991) during the 1990s, have shown that weak synoptic forcing, complex terrain (Fig. 1), and sizable areas void of mesoscale observations are largely to blame for the forecast problems (Haro et al. 1998; Maddox et al. 1993, 1995; McCollum et al. 1995; Hales 1975). It also has been documented that numerical weather prediction (NWP) models provide limited guidance to the forecaster during the monsoon. Dunn and Horel (1994a) showed that in Arizona, the National Centers for Environmental Prediction (NCEP) Nested Grid Model (NGM; Hoke et al. 1989) exhibited no skill in producing quantitative precipitation forecasts (QPFs) during the monsoon, while an earlier 80-km version of NCEP's Eta Model (Janjic 1990, 1994) showed only limited skill by occasionally producing light rainfall over the Arizona deserts, but never predicting precipitation over the mountains or widespread, heavy rainfall events. Lack of Eta Model skill was attributed to a poor representation of the moisture field, convective initiation occurring at scales that the model could not resolve, and an inability of the model to initiate convection over high terrain (Dunn and Horel 1994b). Stensrud et al. (1995) used the Pennsylvania State University–National Center for Atmospheric Research (PSU–NCAR) Mesoscale Model, Version 4, (MM4; Anthes and Warner 1978; Anthes et al. 1987) to produce a one-month model climatology of the monsoon in Mexico. Their model simulation reproduced many of the observed features of the monsoon circulation, such as the large-scale midtropospheric wind fields, southerly low-level winds over the Gulf of California, and heavy rainfall over western Mexico. They emphasized that choosing appropriate physical param-

Corresponding author address: David R. Bright, NOAA/NWS, 520 N. Park Ave., Suite 304, Tucson, AZ 85719-5035.
E-mail: david.bright@noaa.gov

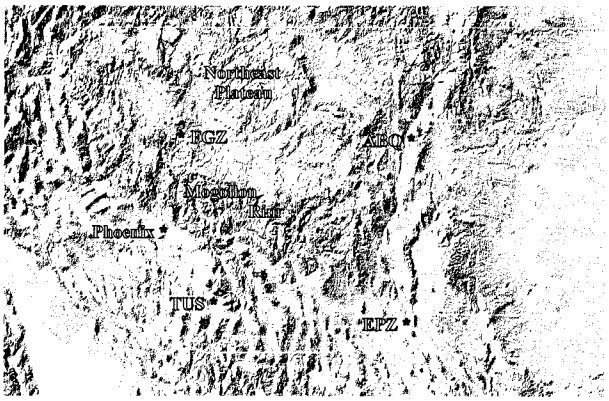

FIG. 1. The topography of the southwest United States. Location of National Weather Service rawinsonde sites Albuquerque, NM (ABQ), Santa Teresa, NM (EPZ), Flagstaff, AZ (FGZ), and Tucson, AZ (TUS) are indicated.

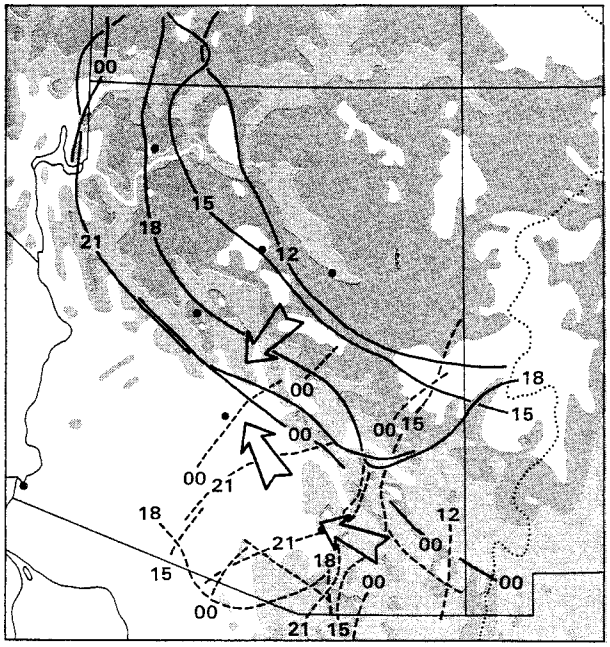

FIG. 2. Isochrones of maximum lightning activity for 1100–0000 LST in 3-h increments. (solid lines) Plateau-generated lighting; (dashed lines) southeast highlands–generated lightning. Taken from Watson et al. (1994).

eterizations is as important as accurate initial conditions. This point was reiterated by Haro et al. (1998) in their review of two Arizona severe thunderstorm events that occurred in August 1996. Winds near Phoenix in excess of 160 km h^{-1} (100 mph) were measured in both events. They noted the inability of synoptic and mesoscale models to forecast properly the evolution of the planetary boundary layer (PBL) as the major impediment to the model's ability to provide useful guidance beyond 12 hours.

This paper focuses on the importance of the PBL evolution to Arizona monsoon convection, and ability of the PSU–NCAR fifth-generation Mesoscale Model (MM5; Grell et al. 1995) to predict its evolution prior to convective events. Section 2 provides background information on the PBL and forecasting convection during the monsoon, and section 3 provides observational examples illustrating some of the challenges faced by Arizona forecasters in sounding analysis for thunderstorm prediction. Emphasis is placed on PBL features that we believe forecasters need to evaluate carefully in order to produce accurate, short-term forecasts. A description of two local, higher-order and two nonlocal PBL schemes included with MM5 version 2 (release 12) is given in section 4. All four of these PBL schemes are considered sophisticated enough for use in MM5 modeling of the monsoon; however, to our knowledge there is no verification published on their ability to reproduce very deep, well-mixed PBLs typical of Arizona and the southwest United States. The methodology of the MM5 PBL experiment is also described in section 4. The results of the experiment are contained in section 5. Section 6 discusses the results, including the suitability of including these PBL schemes in short-term ensembles during the monsoon.

2. Background

a. Forecasting convection during the monsoon

Through operational experience, we believe that careful analysis of observational data, particularly regional soundings, is necessary for making short-term forecasts (i.e., approximately 6 to 18 h) of Arizona convection. Maddox et al. (1995) described how detailed observational analysis can reveal small but significant changes in the severe weather environment of the Southwest. Recently, remotely sensed data such as those from satellites and Weather Surveillance Radar-1988 Doppler (WSR-88D) radars have proved valuable additions to the observational network (e.g., Bright and McCollum 1998). Nevertheless, operational forecasters still rely heavily on climatology to provide the conceptual basis for their short-term forecasts and warnings. Probably the most significant climatological feature of Arizona convection is its correlation with the diurnal cycle and terrain. Cloud-to-ground lightning activity is at a maximum in Arizona at 1600 local standard time (LST) (Watson et al. 1994). Thunderstorms typically begin over the mountains around noon LST and move toward lower terrain during the afternoon and evening hours (Fig. 2), sometimes reaching the central deserts of Phoenix with a peak frequency at 2300 LST (Balling and Brazel 1987).

The deterministic model forecasts completed for this study revealed that 6-to-18-h forecasts of Arizona convection are more challenging in the lower elevation deserts farther removed from the mountains. This is because the model must accurately generate and move the mesoscale forcing for convective initiation away from its high-elevation source and into the lower deserts. The success of the numerical forecast is therefore related to the model PBL evolution, since diurnal changes in the

structure of the PBL directly impact convective available potential energy (CAPE), convective inhibition (CIN), and downdraft convective available potential energy (DCAPE), particularly in the lower elevations. [In this paper, CAPE refers to the positive buoyant energy between the level of free convection and the equilibrium level, while CIN refers to the negative buoyant energy below the level of free convection. All calculations of CAPE and CIN are based on pseudoadiabatic processes (Emanuel 1994) and 60-mb parcel averages unless otherwise stated. DCAPE also follows Emanuel (1994), and represents the maximum potential energy that can be realized in a precipitating downdraft. In this paper DCAPE is calculated by first cooling a parcel just above the lifting condensation level isobarically through a wet-bulb process, and then assuming evaporation maintains saturation during pseudoadiabatic descent.]

b. *Numerically simulating the planetary boundary layer*

The daytime growth of the PBL results from turbulent exchanges, primarily driven by intense surface heating. This growth is principally governed by how the net radiation received at the surface is partitioned into sensible, latent, and soil heat fluxes. Simple bulk models of the PBL (also called slab models and referred to as half-order closure models) assume a priori a vertical distribution of wind, temperature, and/or moisture. Once the wind, temperature, or moisture is known at a point in the PBL, its value at all heights of the PBL is diagnosed. For decades, variations of the bulk method have been used in meteorological models with sufficient accuracy that it remains a popular modeling technique today (Stull 1988; e.g., see Stensrud 1993). However, sophisticated mesoscale models need to include effects of processes internal to the PBL, such as turbulent eddies of various sizes in various stability regimes. These processes are not represented accurately by the conceptual simplicity of bulk parameterizations.

The next level of sophistication beyond the bulk formulation is first-order closure (often called *K*-theory), which assumes that turbulent fluxes flow downgradient in proportion to an eddy diffusivity and the local vertical gradient of the quantity being transferred (Garratt 1992). First-order closure works best for neutral or stably stratified PBLs, but worsens as convection becomes dominant over shear in the production of PBL turbulence. Many mesoscale models now employ PBL parameterizations incorporating higher-order closure schemes, where in addition to prognostic equations for the mean quantities, prognostic equations are also retained for the turbulent fluxes. These higher-order schemes typically determine the turbulent fluxes through values and/or gradients of predicted quantities at the same vertical point. Because the turbulent closure is evaluated at the same vertical grid point, these schemes are referred to as utilizing local closure. Another approach used in mesoscale models is nonlocal closure, where the turbulent fluxes at a point are parameterized by predicted quantities at several vertical points through the depth of the PBL. Nonlocal schemes assume that turbulence is a superposition of eddies of various sizes, and are therefore well suited for parameterizing the effects of large eddies in an unstable, convective PBL. Local schemes have been extended to third order, while nonlocal schemes have been limited to first order (Garratt 1992). See Stull (1988, chapter 6) for a mathematically based discussion on turbulent closure.

c. *Planetary boundary layers in complex terrain*

Anticipating changes in the structure of the PBL is further complicated by vertical growth into a layer of the free atmosphere modified by prior contact with the surface. These elevated residual layers (ERLs) tend to conserve mean state variables of the boundary layer in which they originally formed. Complex terrain and steep terrain gradients make ERLs rather common over the western United States. During the 1990 SWAMP, Stensrud (1993) found ERLs over Phoenix about 20% of the time. An ERL may or may not be well mixed, but a unique and common subset of the ERL is the elevated mixed layer (EML). The EML is a former, well-mixed PBL, often originating over high terrain and subsequently moving over lower terrain, away from its high-elevation heat source and into the free downstream atmosphere. EMLs often act as a ''lid'' on convective storm formation in the central United States (Lanicci and Warner 1991a,b,c; Graziano and Carlson 1987; Carlson et al. 1980, 1983) with the horizontal location of the EML strongly influenced by the interaction of the large-scale flow with the mesoscale environment (Lieman and Alpert 1993). A lid is defined as an EML over a moist PBL, and over the southern Great Plains typically exist for about one week (Lanicci and Warner 1991b).

Stensrud (1993) showed that ERLs influence the potential for convection depending on their characteristics, particularly the gradient of potential temperature separating the ERL from the PBL. He found that if an ERL is separated from the PBL by a strong, shallow inversion (i.e., large vertical gradient of potential temperature), then the surface moisture flux (i.e., latent heating) tends to dominate over dry air entrainment at the top of the PBL. Therefore, if the surface moisture flux is large enough, the water vapor content of the PBL will increase despite its slow growth into a drier ERL. However, if the inversion separating the ERL from the PBL is relatively deep and weak (i.e., small vertical gradient of potential temperature), then ERL air is quickly entrained downward into the PBL, dominating the surface moisture flux. Thus, if the ERL is drier than the PBL, then the entrainment of air from above will dominate the latent heat flux, resulting in a net drying of the PBL. (Typically, the ERL is drier than the PBL, but this is

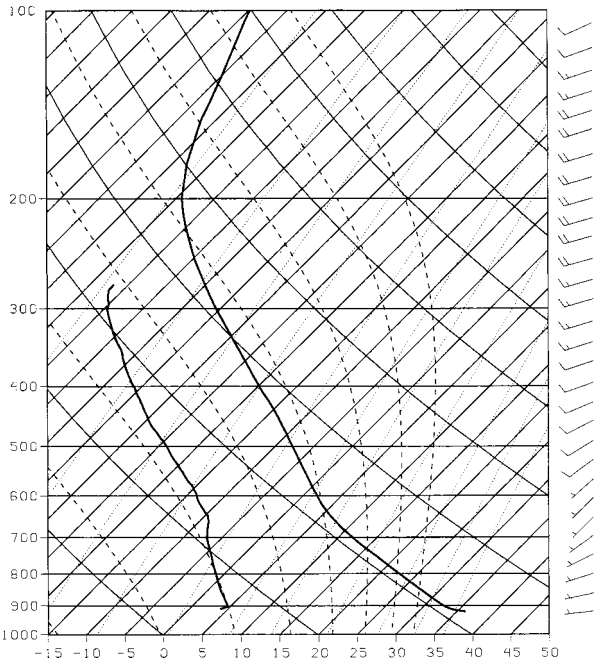

FIG. 3. Skew *T*–log*p* plot of 0000 UTC composite sounding for all dry days at Tucson, AZ, between 10 and 19 Jun 1961–90. Wind in m s^{-1}.

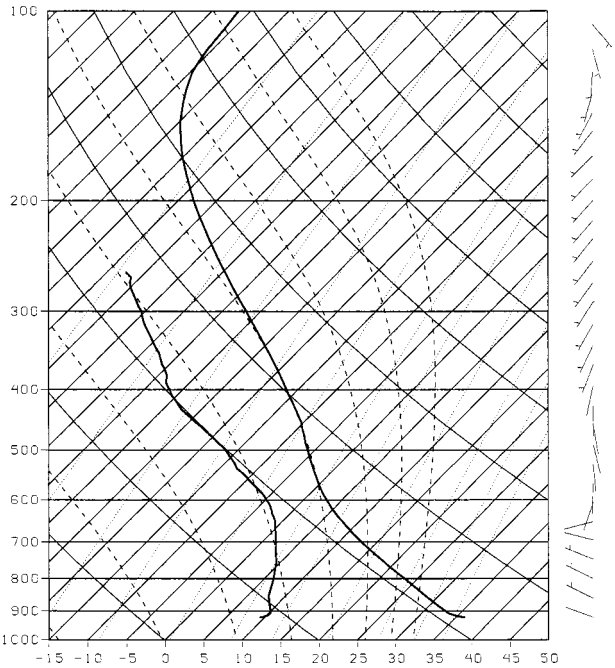

FIG. 4. Skew *T*–log*p* plot of 0000 UTC composite sounding for all dry days at Tucson, AZ, between 10 and 19 Jul 1961–90. Wind in m s^{-1}.

not necessarily true if the ERL was created by moist convection.) In high temporal resolution soundings taken over Phoenix during SWAMP, Stensrud (1993) showed examples of rapidly decreasing CAPE (and increasing CIN) when an ERL moved over the Phoenix PBL.

3. Observations of the desert PBL

Afternoon boundary layers over the desert Southwest grow considerably deeper than other regions of the country (Holzworth 1964). This is particularly true during the late spring and early summer months prior to the monsoon, when minimal vegetation and dry soil allow most of the available insolation to go toward sensible heating. During the monsoon, forecasting changes to the PBL and its conditional instability are considerably more complex. Midtropospheric air entrained into the afternoon PBL is not necessarily dry (Douglas et al. 1993), and an increase in soil moisture resulting from the monsoon rainfall changes the land–surface energy budget.

A 0000 UTC (1700 LST) 30-yr, premonsoon composite sounding at Tucson, Arizona, for all dry days (i.e., all calendar days without trace or measurable precipitation at Tucson International Airport) between 10–19 June 1961–90 contains a precipitable water of 16 mm and a PBL top at approximately 650 hPa (Fig. 3). The mixing ratio decreases rapidly with height through the entire PBL. Winds in the composite sounding are southwest above the PBL, indicating southern Arizona is still under the influence of a relatively dry Pacific air mass, in good agreement with regional monsoon composites (Douglas et al. 1993). An entraining PBL (Stull 1988) can explain the observed drying with height in the boundary layer. One month later and typically during the monsoon, a 30-yr composite sounding of all dry days at Tucson between 10–19 July 1961–90 indicates the top of the PBL has decreased to about 700 hPa, the mixing ratio is more uniformly distributed through the PBL, the precipitable water has increased to 28 mm, with moistening at all levels of the troposphere (Fig. 4).

Elevated heat sources due to rugged topography (see Fig. 1) and strong insolation can produce deep and complex PBLs over Arizona. The 0000 UTC 22 July 2000 sounding over Tucson (Fig. 5) shows a classic EML between 650 and 500 hPa, and evidence of a very shallow EML between 670 and 650 hPa. These EMLs likely formed as PBLs over the mountain ranges east of Tucson and advected westward over the lower elevation PBL. The mixing ratio of the EML between 650 and 500 hPa is a uniform 3.1 g kg^{-1}, while the mixing ratio of the Tucson PBL is considerably higher at 7.5 g kg^{-1}. The strong inversion separating the PBL from the deep EML suggests that the entrainment of dry air will proceed slowly. One can then deduce that a rapid decrease (increase) in the 653 J kg^{-1} of surface parcel CAPE (56 J kg^{-1} of CIN) is unlikely; although, a substantial amount of CIN must be overcome to initiate convection. Outflow from thunderstorms that originated over the Mogollon Rim and White Mountains around 2200 UTC

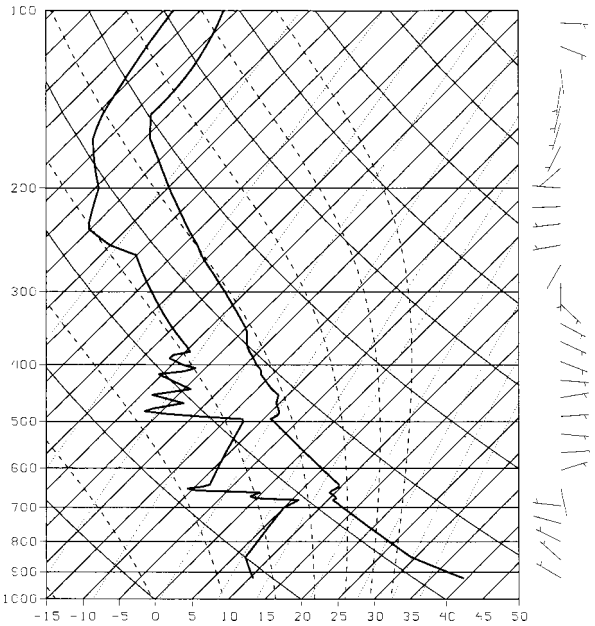

FIG. 5. Skew *T*–log*p* plot of sounding at Tucson, AZ, 0000 UTC 22 Jul 2000. Wind in m s^{-1}.

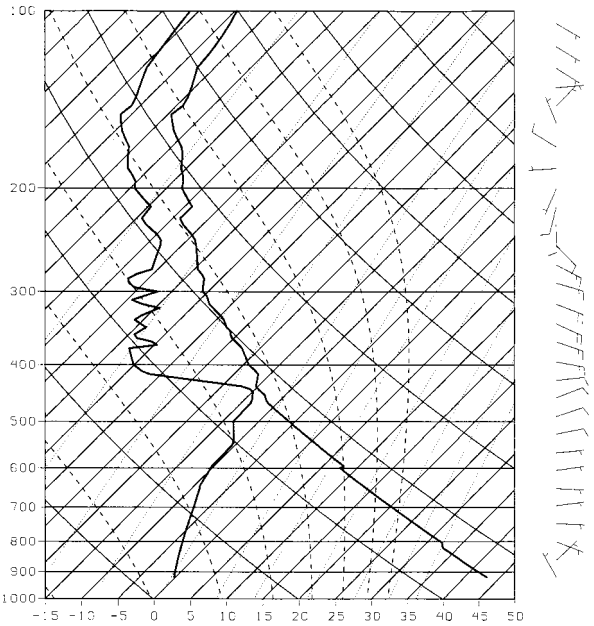

FIG. 6. Skew *T*–log*p* plot of sounding at Tucson, AZ, 0000 UTC 29 Jul 1995. Wind in m s^{-1}. (Unrealistically high dewpoint temperatures below 700 hPa and above the surface were removed from the plot.)

triggered thunderstorms in the Tucson area between 0300 and 0400 UTC [according to National Weather Service (NWS) Tucson surface observations and storm log].

After days of intense heating and the complete entrainment of EMLs into the PBL, extremely deep PBLs can form, such as the 0000 UTC (1700 LST) 29 July 1995 Tucson sounding shows (Fig. 6). The PBL reaches 470 hPa (the small inversions at 800 and 600 hPa appear spurious) and the mixing ratio is reasonably well mixed but only about 3 g kg^{-1} (erroneously high dewpoint temperatures above the surface and below 700 hPa were removed). This environment is very similar to the Western dry-microburst environment described by Wakimoto (1985). Because a large amount of DCAPE exists in the environment (about 2300 J kg^{-1} for a parcel originating at 450 hPa), and the cloud base is well above the freezing level, even a shallow precipitating cloud in the 450–300-hPa layer is capable of generating a strong downdraft (Proctor 1989; Emanuel 1994). Indeed, isolated high-based convection developed over the Phoenix, Arizona, metropolitan area (160 km northwest of Tucson) around 0400 UTC (2100 LST), producing measured wind gusts to 115 km h^{-1} (70 mph) and numerous reports of wind damage, but very little rainfall (NCDC 1995; Green and Haro 1998). A heat burst (Johnson 1983), which is an abrupt increase in surface temperature as a precipitation-induced downdraft penetrates the shallow nocturnal inversion, occurred at Sky Harbor International Airport at 0600 UTC (2300 LST) when the temperature jumped to 46°C (114°F). Although reports of cloud-to-cloud lightning were frequent, no cloud-to-ground lightning accompanied the storms in the Phoenix metropolitan area (R. Holle, Global Atmospherics, Tucson, AZ, 2001, personal communication).

An interesting event that illustrates the complexity and sensitivity of the desert PBL to convective initiation occurred 29 June 2000. The 1200 UTC (0500 LST) sounding at Phoenix [Fig. 7; C. Dempsey, Salt River Project (SRP), Tempe, AZ, 2001, personal communication] will become conditionally unstable as the PBL develops during the day. The 1200 UTC Tucson sounding was of minimal value to the forecasters due to convective contamination (i.e., the Tucson sounding sampled the residual effects of nocturnal convection not representative of the large-scale environment). An EML is situated over Phoenix between 750 and 600 hPa, with an ERL between about 810 and 750 hPa. Based on the uniform northeast wind at about 10 m s^{-1}, the EML could have formed the previous afternoon as the PBL over the northeast Arizona plateau (about 400 km northeast of Phoenix), with the lower portion perhaps modified by nocturnal cooling, forming an ERL, as it passed over the Mogollon Rim (about 150 km northeast of Phoenix). (The formation of the EML/ERL is indeed speculative; however, its existence and not its origin is the topic of discussion.) The sounding presents a difficult challenge to the forecaster, since afternoon instability is dependent upon how the developing PBL and drier ERL/EML interact. The threat for severe convection was significant enough to prompt the Storm Prediction Center, in coordination with Arizona NWS of-

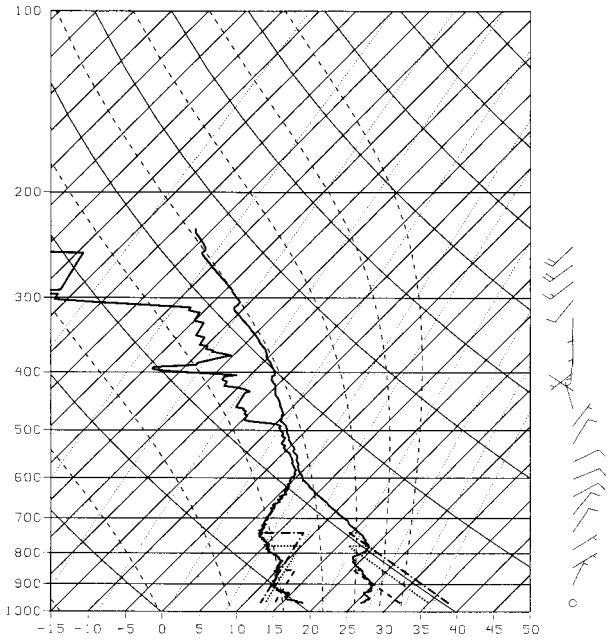

FIG. 7. Skew *T*–log*p* plot of sounding at Phoenix, AZ, 1200 UTC 29 Jun 2000 (solid) and PBL forecast sounding valid at 1600, 2000, and 0000 UTC (dash, dot, dash–dot, respectively) using a one-dimensional bulk model. Wind at 1200 UTC in m s^{-1}.

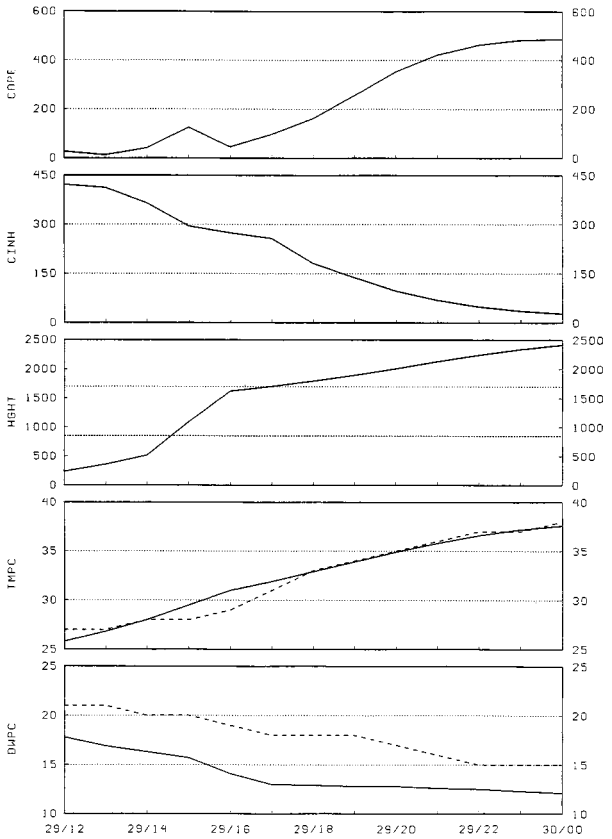

FIG. 8. (top to bottom) Meteograms of forecast CAPE (J kg^{-1}), CIN (J kg^{-1}), PBL height (m), surface temperature (°C), and surface dewpoint (°C), using the one-dimensional bulk model. The dashed lines in the lower two panels represent the observed temperature and dewpoint, respectively, from nearby Sky Harbor International Airport.

fices, to issue a severe thunderstorm watch for much of central Arizona at 2000 UTC (1300 LST).

A one-dimensional bulk PBL model (Stull 1988, p. 456) driven by a simple parameterization of the net radiative flux (Stull 1988, 256–259) is used to estimate the development of the Phoenix PBL and its conditional instability. The model assumes a constant entrainment coefficient, partly cloudy sky cover (two-tenths mid- and high-level cloud, respectively), and a constant Bowen ratio (ratio of sensible to latent surface heat fluxes). The value of the Bowen ratio and entrainment coefficient are 4.5 and 0.2, respectively, and are considered representative of a free-convective PBL in a semiarid environment (Stull 1988, pp. 274, 478). The latent heat flux is simply determined using the assumed Bowen ratio. Day-to-day changes in the spatial variability of soil moisture can have a significant impact on the surface energy budget, CAPE, and CIN. Boundaries resulting from differential heating owing to gradients in the soil moisture may be important in convective development (Gallus and Segal 2000; Chang and Wetzel 1991), but this model was simply designed to provide first-order estimates of how CAPE and CIN evolve relative to the growing PBL.

Model output indicates that temperatures warm steadily between 1200 UTC and 2000 UTC (0500 to 1300 LST), while the surface dewpoint steadily decreases as the boundary layer grows into the drier air above the surface (Fig. 7, dash, dot, dash–dot valid at 1600, 2000, and 0000 UTC, respectively). By 2000 UTC the PBL has grown into the ERL, with a strong inversion capping the PBL and slowing the rate of dry air entrainment. The hourly model output plotted as a meteogram (Fig. 8) indicates the forecast CAPE (60-mb surface parcel) is generally quite low through 1600 UTC (0900 LST), and then steadily increases as heating continues but dry air entrainment slows as the PBL grows into the ERL above 810 hPa. CAPE values never become very large, and peak at just under 500 J kg^{-1} around 0000 UTC (1700 LST). CIN is predicted to decrease through the day, but remains an appreciable 30 J kg^{-1} during the late afternoon, indicating convection in the Phoenix valley is unlikely without a strong outflow. The model simulation of CAPE and CIN seems credible based on the good agreement of the predicted surface temperature to the observed surface temperature at nearby Sky Harbor International Airport. The dewpoint trend is also forecast quite well, but the model dewpoint (using 1200 UTC SRP data for initialization) is always less than the Sky Harbor International Airport dewpoint. In this case, convection did not overcome the EML lid in the central deserts (in good agreement with the bulk model prediction), and no severe weather occurred in the Phoenix metropolitan area (NCDC 2000).

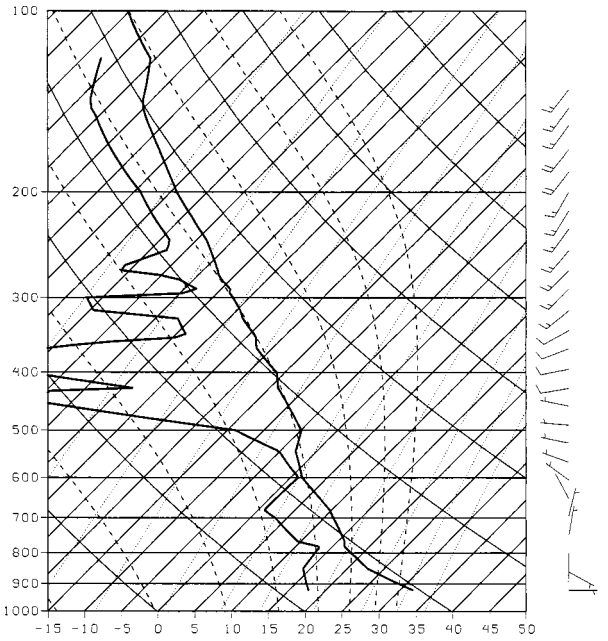

FIG. 9. Skew *T*–log*p* plot of sounding at Tucson, AZ, 0000 UTC 30 Jun 2000. Wind in m s^{-1}.

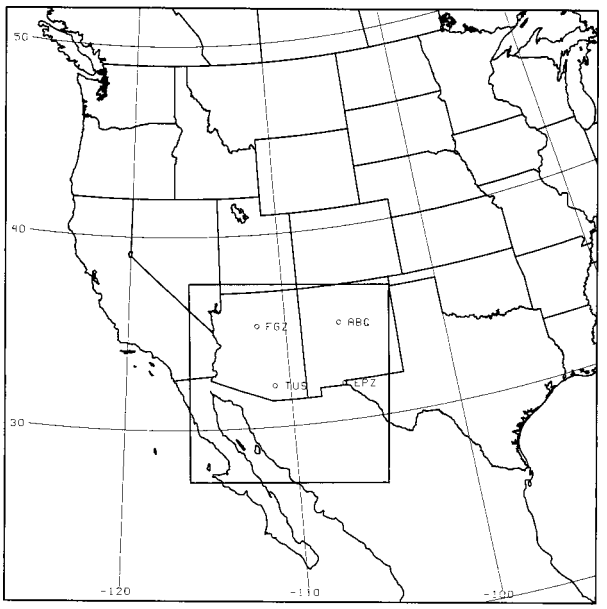

FIG. 10. Location of MM5 54-km coarse domain and 18-km nested domain. Location of National Weather Service rawinsonde sites Albuquerque, NM (ABQ), Santa Teresa, NM (EPZ), Flagstaff, AZ (FGZ), and Tucson, AZ (TUS) are indicated.

During this time, an interesting situation was developing farther south over Tucson. The Tucson sounding at 0000 UTC (1700 LST) 30 June shows an ERL with a top at 600 hPa and base around 680 hPa (Fig. 9). The top of the ERL and its mean potential temperature and mixing ratio (316 K and 6 g kg^{-1}, respectively) are nearly identical to those observed in the EML over Phoenix earlier in the day; however, the winds are now north at 5 m s^{-1}. This ERL may have originated from the EML observed over Phoenix earlier in the day, or perhaps formed over the Santa Catalina mountains just north of Tucson. In any event, cloud cover earlier in the day and moist soil from recent rainfall limited the growth of the Tucson afternoon PBL to only 780 hPa, well below the base of the ERL. Low-level moisture advection in combination with the warm air below the ERL (between 700 and 650 hPa) capped convective initiation (CIN 39 J kg^{-1}) during the afternoon hours, allowing a considerable amount of conditional instability to form over Tucson (CAPE 1192 J kg^{-1}). At 0400 UTC (2100 LST) the lid was overcome as a small complex of thunderstorms developed over southern Arizona. The storms that developed in the Tucson metropolitan area produced urban flash flooding (up to 6 cm of rain between 0400 and 0600 UTC) but no reports of severe wind or hail (NCDC 2000).

4. Numerical simulation of the desert PBL using MM5

The Tucson NWS office, in cooperation with the University of Arizona, has performed real-time MM5 forecasts since the summer of 1997 (see Farfan et al. 1998, 2000). Initial sensitivity studies showed that different PBL parameterizations produced notably different forecasts; however, we could find no existing study of MM5 PBL performance in Arizona during the monsoon. In related climate work, Giorgi et al. (1993) found that a nonlocal PBL scheme favorably decreased the amount of convective precipitation due to more rapid upward mixing of low-level moisture, while Holtslag and Boville (1993) noted that a nonlocal PBL scheme showed promise because it (more correctly) transferred moisture away from the surface than a local scheme. This present study was conducted to determine the most appropriate MM5 PBL parameterization(s) to use for deterministic and ensemble modeling of the monsoon. The four MM5 PBL parameterizations tested were the Blackadar (BLK; Zhang and Anthes 1982). Burk–Thompson (BT; Burk and Thompson 1989), Eta (Janjic 1994), and the MRF (Hong and Pan 1996) schemes.

a. The four MM5 PBL parameterizations

1) BLACKADAR PBL PARAMETERIZATION

The high-resolution boundary layer scheme based on Blackadar (1976, 1978) and Zhang and Anthes (1982) is used to forecast the vertical mixing of horizontal wind, potential temperature, mixing ratio, cloud water, cloud ice, and graupel. The stable, nocturnal regime and free-convective regime are treated differently. In the nocturnal regime, the atmosphere is stable (or marginally unstable) and turbulence is the result of mechanical processes, while in the free-convective regime the atmosphere is unstable and turbulence is the result of free-

TABLE 1. Bias (model − observation) and standard deviation (shown in parentheses) of the initial model vertical profile at 1200 UTC for the 21-day period in Aug 1998. A positive (negative) bias indicates the model is greater (less) than the observation.

Site	Temp (°C)	r (g kg^{-1})	u (m s^{-1})	v (m s^{-1})
ABQ	−0.4 (1.0)	−0.3 (0.4)	0.1 (1.2)	−0.6 (1.3)
EPZ	−0.5 (0.8)	−0.1 (0.4)	0.3 (1.2)	−0.7 (1.1)
FGZ	−0.4 (1.6)	0.1 (0.7)	−0.2 (2.3)	−0.3 (1.4)
TUS	−0.9 (1.6)	0.3 (0.8)	0.0 (1.2)	0.1 (1.1)
All	−0.6 (1.3)	0.0 (0.6)	0.1 (1.5)	−0.3 (1.3)

TABLE 2. Bias (model − observation) and standard deviation (shown in parentheses) of the 12-h forecast model vertical profile valid at 0000 UTC for the 21-day period in Aug 1998 using the BLK PBL parameterization. A positive (negative) bias indicates the model is greater (less) than the observation. Bold numbers indicate the smallest bias or std dev among the four PBL schemes.

Site	Temp (°C)	r (g kg^{-1})	u (m s^{-1})	v (m s^{-1})
ABQ	0.1 (1.0)	−1.1 (1.5)	−0.4 (2.4)	0.9 (3.2)
EPZ	0.1 (1.7)	0.1 (1.6)	−0.6 (2.8)	−0.1 (2.1)
FGZ	−0.4 (1.5)	0.8 (1.4)	−1.5 (3.7)	0.1 (3.4)
TUS	0.6 (1.1)	0.3 (1.4)	−1.4 (2.5)	0.8 (2.0)
All	**0.1 (1.4)**	**0.0** (1.7)	**−1.0** (2.9)	0.5 (**2.8**)

convective thermals of warm, rising air. In the nocturnal regime, a first-order closure approach based on *K*-theory is used to determine the turbulent fluxes. Because the nocturnal regime is a local scheme, mixing is assumed to occur only between adjacent model layers. In contrast, the free-convective regime employs a nonlocal approach where buoyant plumes of warm air are assumed to mix heat, moisture, and momentum at every level of the mixed layer.

2) BURK–THOMPSON PBL PARAMETERIZATION

The BT scheme available in MM5 is based on its initial implementation in the Navy Operational Regional Atmospheric Prediction System (NORAPS; Burk and Thompson 1989). The scheme parameterizes PBL turbulence through local, second-order closure based on Mellor and Yamada's (1974) level 3 model. In MM5, the scheme is used to forecast the vertical mixing of horizontal wind, potential temperature, mixing ratio, cloud water, and rainwater through prognostic equations for turbulent kinetic energy, temperature variance, moisture variance, and temperature–moisture covariance. All other fluxes are obtained diagnostically. Its inclusion of prognostic equations for the higher statistical moments allows for the simulation of well-mixed PBLs, but at increased computational expense.

3) ETA PBL PARAMETERIZATION

The Eta PBL parameterization in MM5 is based on implementation of Mellor and Yamada's (1974) level 2.5 model in the NCEP Eta Model (Janjic 1994). It is a local, one-and-a-half order closure scheme in the PBL with a prognostic equation for turbulent kinetic energy. In MM5, the scheme is used to forecast the vertical mixing of horizontal wind, potential temperature, and mixing ratio.

4) MRF PBL PARAMETERIZATION

The MRF PBL parameterization (Hong and Pan 1996) is a first-order, nonlocal scheme based on the results of the large-eddy simulations by Wyngaard and Brost (1984). It represents large-eddy turbulence in a well-mixed PBL, and is computationally the most economical. It has been used in general circulation models and numerical weather prediction models because of its computational efficiency and its ability to simulate large-eddy turbulence in well-mixed PBLs. In MM5, the scheme is used to forecast the vertical mixing of horizontal wind, potential temperature, mixing ratio, cloud water, cloud ice, and graupel.

b. Methodology

The model was initialized at 1200 UTC (0500 LST) during 21 days of August, 1998. Four, 12-h forecasts were produced daily, each forecast containing a different PBL scheme. Verification data consisted of the four operational NWS rawinsondes available in the southwest United States [Flagstaff, AZ (FGZ); Albuquerque, NM (ABQ); Tucson, AZ (TUS); Santa Teresa, NM (EPZ); see Fig. 1 or Fig. 10 for locations]. The forecast duration was 12 h to examine the predicted afternoon PBL as compared to 0000 UTC (1700 LST) soundings.

The MM5 model was configured with 27 layers in the vertical, a 64 × 64 gridpoint coarse domain at 54-km grid spacing, and a 64 × 64 gridpoint, two-way interactive nest at 18-km grid spacing (Fig. 10). Output from the 18-km nested domain was used for all model verification. Model physics include the simple explicit microphysical parameterization for cloud water and rainwater below the freezing level, and cloud ice and snow above the freezing level (Grell et al. 1995; Dudhia 1989; Zhang 1989), the Kain–Fritsch convective parameterization (Kain and Fritsch 1990, 1993), a five-layer soil temperature model with fixed substrate (Dudhia 1996), and a cloud radiation scheme accounting for longwave and shortwave radiative transfer in cloudy and clear air (Grell et al. 1995; Dudhia 1989). Terrain height and land-use information for the 18-km domain were derived from the NCAR 10-min (approximately 19 km) global terrain and land-use database. Initial and lateral boundary conditions were interpolated directly from NCEP's Eta Model available on Advanced Weather Interactive Processing System (AWIPS) grid 211 (80-km grid spacing; Stackpole 1994) to the MM5 grid. To overcome a dry bias over Arizona in the low levels of the Eta initial moisture fields (Farfan et al. 1998), a locally developed reanalysis scheme nudged 1200 UTC initial grids of interpolated temperature and moisture (below

TABLE 3. As in Table 2 except using the BT PBL parameterization.

Site	Temp (°C)	r (g kg^{-1})	u (m s^{-1})	v (m s^{-1})
ABQ	−0.7 (1.3)	−0.7 (1.6)	−0.4 (3.4)	−0.1 (3.5)
EPZ	−1.3 (1.7)	1.2 (2.1)	−1.1 (3.0)	−0.1 (2.5)
FGZ	−1.3 (1.7)	1.5 (2.0)	−1.0 (3.4)	−0.3 (3.4)
TUS	−0.7 (1.5)	1.5 (2.4)	−1.9 (2.7)	1.4 (2.1)
All	−1.0 (1.6)	0.8 (2.3)	−1.1 (3.2)	**0.3** (3.0)

TABLE 4. As in Table 2 except using the Eta PBL parameterization.

Site	Temp (°C)	r (g kg^{-1})	u (m s^{-1})	v (m s^{-1})
ABQ	−0.7 (1.5)	−0.4 (1.5)	−0.6 (2.7)	0.3 (3.4)
EPZ	−1.2 (1.8)	1.3 (1.7)	−1.0 (2.8)	−0.1 (2.1)
FGZ	−1.1 (1.6)	1.2 (1.8)	−1.2 (3.4)	−0.1 (3.2)
TUS	−0.4 (1.4)	1.1 (2.1)	−2.1 (2.6)	1.3 (2.0)
All	−0.9 (1.6)	0.8 (2.0)	−1.2 (2.9)	0.4 (2.8)

700 hPa) toward observed 1200 UTC upper air and surface observations. In the MM5 preprocessing system, the initial ground temperature is set to the initial surface temperature. Soil moisture availability is simply assigned its climatological summertime value based on the land-use category at the particular grid point.

Verification of the model's PBL forecast consisted of comparing the model forecast vertical profile (i.e., forecast sounding) against the four rawinsonde observations. To avoid introducing additional uncertainty due to interpolation, the forecast soundings were extracted directly from the grid point nearest the observation site. Comparisons were made at the initial time (1200 UTC) to quantify the accuracy of the initial conditions, and after the 12 h forecast (valid 0000 UTC) to verify the accuracy of the PBL forecast.

Prior to the statistical analysis, all 0000 UTC and 1200 UTC soundings (model and observed) were visually inspected for either convective contamination or erroneous data. Convective contamination constitutes any sounding we believe was not representative of the large-scale, preconvective PBL due to localized convection or organized convective systems (e.g., ''onion'' soundings; Zipser 1977). Any real or predicted sounding showing evidence of occurring, recent, or nearby convection, or spurious data, was removed from the 21-day statistical analysis; eight of the 84 possible soundings were removed in this way. With the exception of integrated quantities such as CAPE and CIN, verification consisted of all observed sounding data being vertically interpolated to the nine lowest MM5 sigma layers. The lowest sigma layer (0.995) was always removed from the analysis to ensure that any spurious surface effects would not contaminate the results. [For example, the NWS Automated Surface Observing System (ASOS) uses ''chilled mirror'' technology (for ASOS information, see http://www.nws.noaa.gov/asos) to determine the dewpoint temperature. Personal experience in Tucson has shown that the mirror must be cleaned frequently during the summer months to ensure accurate dewpoint measurements in the desert. Rather than subjectively determining the validity of the observed surface dewpoint temperatures, all surface data were simply removed from the analysis.] At the four verification sites, the top (ninth) sigma layer used for verification ranged from 170 to 200 hPa above the surface, which is generally near the top of the afternoon PBL in the Southwest. Although the PBL often exceeds 170 to 200 mb depth, the analysis was restricted to this layer to ensure the results reflect the properties of the PBL and not the free atmosphere above.

5. Results

The accuracy of the MM5 initial analysis compared to the rawinsonde observation indicates a slight cool bias (−0.6°C) in the model initial conditions when all four sites are considered collectively (Table 1). The largest MM5 cool bias is found at TUS (−0.9°C) and the smallest at ABQ and FLG (−0.4°C). The vertical profile of mixing ratio r shows no initial bias (0.0 g kg^{-1}) when all sites are considered, with individual biases ranging from a slight MM5 dry bias at ABQ (−0.3 g kg^{-1}) to a slight MM5 wet bias at TUS (0.3 g kg^{-1}). The MM5 bias for the u and v component of the wind is also small (0.1 m s^{-1} and −0.3 m s^{-1}, respectively) when all four sites are considered collectively.

Similar statistics at the 12-h forecast time (valid 0000 UTC) were computed for the BLK, BT, Eta, and MRF PBL parameterizations (Tables 2 through 5, respectively. The bold numbers in the ''All'' row indicate the smallest bias or standard deviation among the four PBL schemes.) The BLK PBL scheme (Table 2) shows the smallest overall temperature bias (0.1°C) and mixing ratio bias (0.0 g kg^{-1}) with the MRF PBL parameterization (Table 5) a close second. In fact, the 12-h forecast accuracy of temperature by both the BLK and MRF PBL schemes is generally as good or better than at initialization (compare Tables 2 and 5 to Table 1); however, the standard deviation is always greater after the 12-h forecast, indicating more variability and error growth exists in the forecast. The mixing ratio also maintains a high degree of accuracy during the 12-h forecast when the BLK and MRF PBL schemes are used. Considering all sites, the BT (Table 3) and Eta (Table 4) PBL schemes show a relatively large cool (−1.0°C and −0.9°C, re-

TABLE 5. As in Table 2 except using the MRF PBL parameterization.

Site	Temp (°C)	r (g kg^{-1})	u (m s^{-1})	v (m s^{-1})
ABQ	0.4 (1.1)	−1.1 (1.5)	−0.7 (2.4)	0.9 (3.1)
EPZ	0.5 (1.8)	0.2 (1.5)	−0.7 (2.5)	0.0 (1.9)
FGZ	−0.2 (1.5)	0.9 (1.2)	−1.4 (3.4)	0.1 (3.3)
TUS	0.9 (1.1)	0.2 (1.3)	−1.2 (2.4)	1.0 (2.1)
All	0.4 (**1.4**)	0.1 (**1.6**)	**−1.0 (2.7)**	0.5 (**2.8**)

TABLE 6. Average pressure (hPa) of the 12-h forecast boundary layer top and its observed value at 0000 UTC for the 21-day period in Aug 1998. The Yes or No in parentheses indicates whether the difference in the forecast PBL top from the observed PBL top is statistically significant at the 5% level. The numbers in bold are the closest to observation.

Site	BLK	BT	Eta	MRF	Observed
ABQ	**596** (No)	633 (Yes)	663 (Yes)	581 (No)	599
EPZ	**650** (No)	723 (Yes)	719 (Yes)	635 (No)	671
FGZ	631 (No)	685 (Yes)	688 (Yes)	**617** (No)	614
TUS	684 (No)	763 (Yes)	733 (Yes)	**646** (No)	658
All	**639** (No)	699 (Yes)	699 (Yes)	618 (No)	633

spectively) and wet (both 0.8 g kg^{-1}) bias, and an obvious decrease in the accuracy (bias) and precision (standard deviation) of the PBL temperature and mixing ratio forecast as compared to the BLK and MRF schemes. In fact, the only site where a local scheme (BT or Eta) temperature bias is less than either nonlocal scheme (BLK or MRF) is at TUS, where the Eta temperature bias (0.4°C) is the smallest among all four PBL parameterizations. However, a large wet bias (1.1 g kg^{-1}), much larger than the BLK or MRF schemes (0.3 and 0.2 g kg^{-1}, respectively), negates the relatively good temperature forecast at TUS. For all four sites, the BLK scheme has the smallest bias, while the MRF scheme generally shows less variability than the other three PBL schemes.

The results of Tables 2 through 5 indicate that the higher-order, local PBL schemes (BT and Eta) produce a monsoon PBL that is too cool and too wet, suggesting that the vertical growth of the PBL is probably too shallow. To quantitatively examine the depth of the PBL, its top was calculated for each observed and model forecast sounding. Here, the top of the PBL is defined as the pressure of the first sigma layer where the potential temperature is 1°C greater than the potential temperature of the second sigma layer. (Again, the lowest sigma layer is neglected to avoid any nonrepresentative surface effects.) The results indicate that the BLK and MRF schemes more accurately predict the depth of the afternoon PBL (Table 6). In MM5, the BT and Eta schemes always forecast a PBL top lower than observed. A test for statistical significance (two-tailed *t*-test, 5% significance level; Wilks 1995, 117–129) found that the difference in forecast versus observed PBL depth is always significant when the BT or Eta PBL schemes are used (Yes in Table 6), but is not significant when the BLK or MRF schemes are used (No in Table 6).

Composite soundings at the Arizona stations graphically illustrate the biases described above. At TUS (elevation 779 m), the composite sounding shows the BT (Fig. 11b) and Eta (Fig. 11c) tendency to produce shallow, cool, and moist PBLs when overlaid with the observed composite. The BLK (Fig. 11a) and MRF schemes (Fig. 11d) more accurately predict the general structure of the PBL; although, none of the schemes predict the light northwest winds observed near the surface. At FLG (elevation 2192 m) the BLK (Fig. 12a) and MRF (Fig. 12d) schemes fit the observed composite better than the BT (Fig. 12b) and Eta (Fig. 12c) schemes. But, the BLK and MRF PBL moisture profile, albeit better than the BT and Eta, is clearly too moist at this high-elevation station. All of the schemes predict too much of a southerly component in the near-surface winds at FLG.

Since the depth of the PBL affects the vertical distribution of heat and moisture in the lower atmosphere, the amount of CAPE, CIN, and DCAPE will vary depending on the PBL parameterization used in MM5. Furthermore, many convective parameterizations employ a trigger function that is explicitly or implicitly based on the amount of CIN (e.g., see Kain and Fritsch 1992). To examine how each PBL forecast might affect the potential for convection, calculations were made of the forecast and observed CAPE and CIN. Computation of CAPE and CIN were based on the average thermodynamic properties of 60-hPa-deep layers lifted from the lowest four sigma layers of the model, similar to the technique used by the Kain–Fritsch convective parameterization (Kain and Fritsch 1993; Fritsch and Kain 1993). (All 27 sigma layers were considered in the calculation of forecast and observed integrated thermodynamic quantities.) The BLK and MRF PBL schemes predict CAPE more accurately than the Eta and BT

TABLE 7. Average of the 12-h forecast CAPE (J kg^{-1}) and its observed value at 0000 UTC for the 21-day period in Aug 1998. The calculations are based on a 60-hPa-deep parcel with its base at the sigma level shown. The Yes or No in parentheses indicates whether the difference in the forecast CAPE from the observed CAPE is statistically significant at the 5% level. The numbers in bold are the closest to observation if the departure from observations is not statistically significant.

Site	Sigma layer	BLK	BT	Eta	MRF	Observed
All	1	148 (Yes)	494 (Yes)	412 (Yes)	151 (Yes)	240
All	2	**130** (No)	407 (Yes)	341 (Yes)	**130** (No)	177
All	3	**125** (No)	373 (Yes)	315 (Yes)	123 (No)	158
All	4	110 (No)	272 (Yes)	246 (Yes)	**112** (No)	116

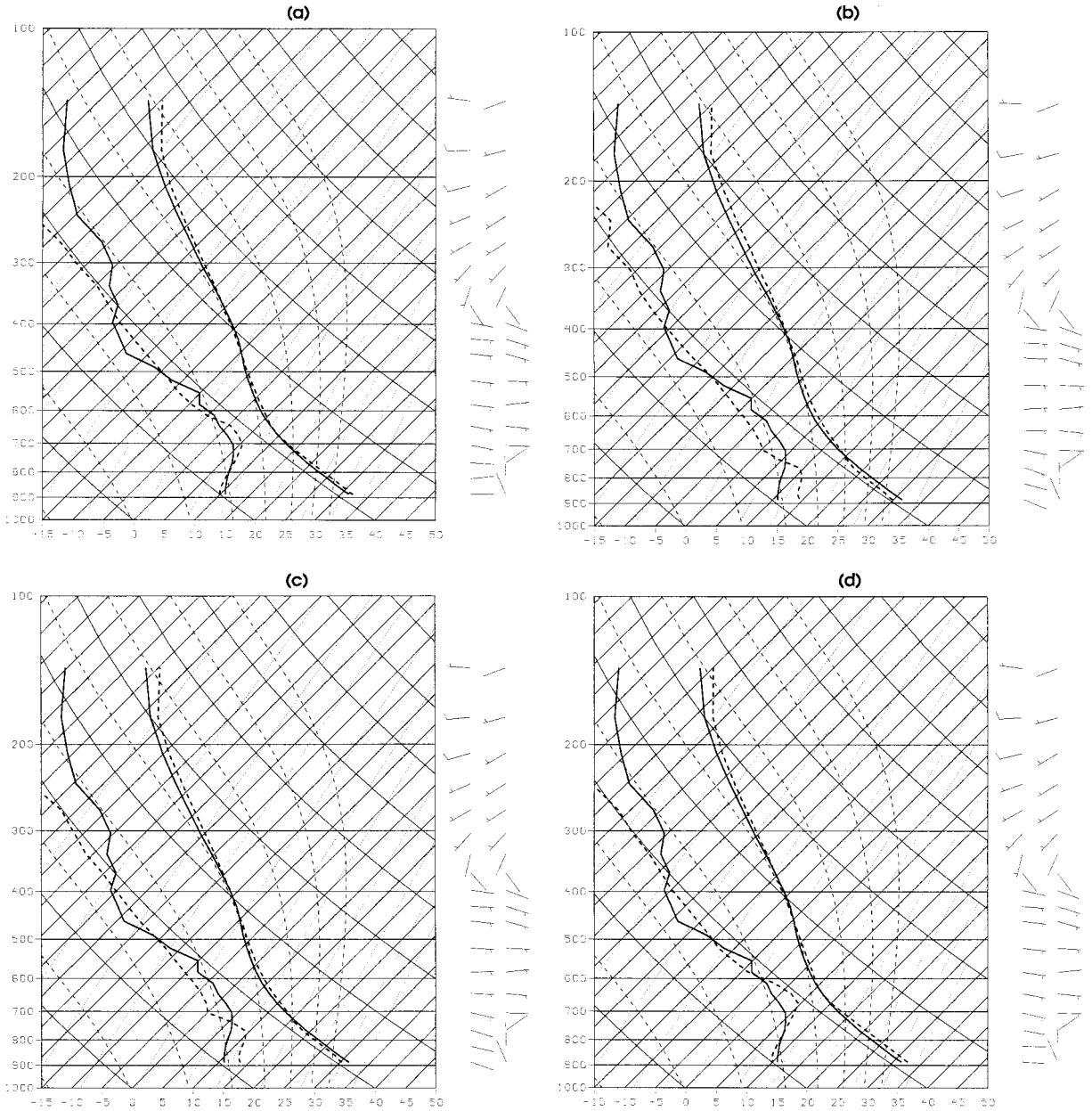

FIG. 11. Skew *T*–log*p* plot of 0000 UTC observed (solid, wind in the right column) and 12-h forecast (dash, wind in the left column) composite sounding at Tucson, AZ, for the (a) BLK, (b) BT, (c) Eta, and (d) MRF PBL schemes. Wind in m s^{-1}.

schemes (Table 7). CAPE based on a parcel with its base at the lowest sigma layer (sigma = 1 in Table 7) was more accurately modeled by the BLK and MRF schemes, but the difference from observation is statistically significant regardless of the scheme used. (Observed surface data is probably affecting the calculation of CAPE here, since the lowest sigma layer was retained in these calculations.) Parcels originating at sigma layers two, three, and four reveal that the BLK and MRF schemes forecast CAPE values closer to observation than the BT and Eta schemes, with differences that are not significant. In MM5, the BT and Eta schemes generally overpredict the CAPE by a significant amount, while the BLK and MRF schemes underpredict the CAPE by a lesser, insignificant amount. The midboundary layer equivalent wet-bulb potential temperature predicted by the BT and Eta schemes is typically about 1°C greater than observation (and the BLK and MRF predictions), consistent with their tendency to overpredict CAPE.

A similar calculation was repeated for the CIN (Table 8). Results are generally less definitive than for CAPE, as all but one test (MRF scheme at sigma = 1) show differences that are statistically significant. In all cases,

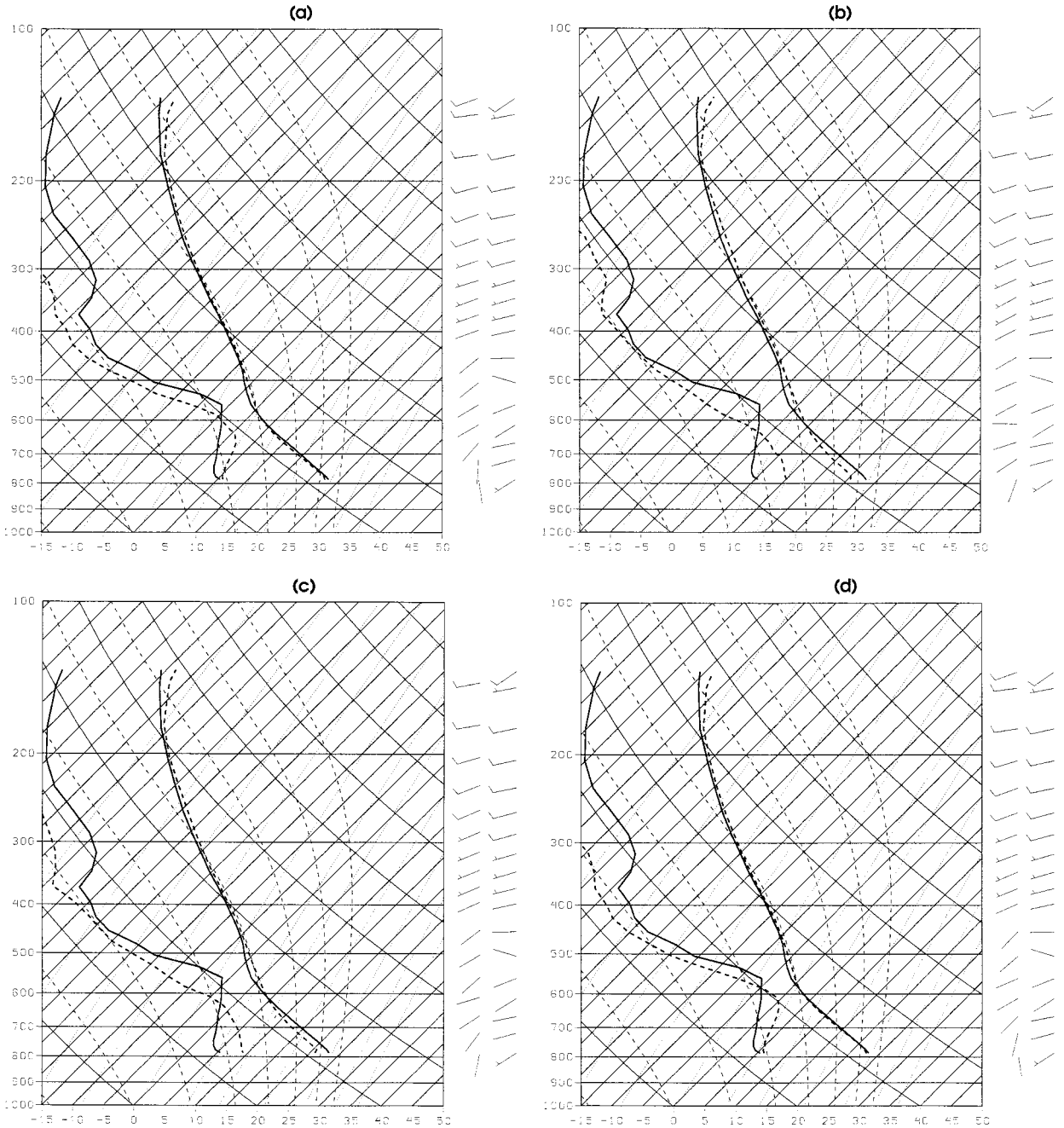

FIG. 12. As in Fig. 11 except for Flagstaff, AZ.

the amount of CIN is underpredicted. The current version of the Kain–Fritsch convective parameterization in MM5 employs a trigger function based on the difference in temperature between the parcel and the environment at the parcel's lifting condensation level, hereafter DTLCL (Fritsch and Kain 1993; Kain and Fritsch 1993). A calculation of DTLCL was made to determine if the BLK or MRF PBL schemes, which forecast CAPE accurately but not CIN, also underpredict the DTLCL (Table 9). In this case, the Eta PBL scheme produces the most accurate result, and it is the only scheme not significantly different from observations; however, due to the cool, moist bias of its predicted PBL, the Eta LCL will tend to be too low. Of more significance is the fact that the BLK and MRF schemes tend to underpredict the DTLCL.

Convective downdrafts and outflow are critically important to the development of new convection during the monsoon (McCollum et al. 1995; Dunn and Horel 1994b; Smith and Gall 1989), so calculations of DCAPE

TABLE 8. As in Table 7 except for CIN (J kg^{-1}).

Site	Sigma layer	BLK	BT	Eta	MRF	Observed
All	1	22 (Yes)	22 (Yes)	24 (Yes)	**28** (No)	37
All	2	19 (Yes)	22 (Yes)	22 (Yes)	24 (Yes)	37
All	3	17 (Yes)	22 (Yes)	21 (Yes)	21 (Yes)	36
All	4	15 (Yes)	**25** (No)	23 (No)	18 (Yes)	31

were also made to determine if a particular PBL scheme can better predict the potential intensity of downdrafts (Table 10). These calculations were based on moist descent from the sigma layer just above the LCL (parcel averages were not used in the calculation of DCAPE). The BLK and MRF schemes yield more accurate calculations of DCAPE, with differences that never differ significantly from observation. The BT and Eta schemes tend to show significantly different amounts of DCAPE than observed.

6. Discussion and summary

The prediction of monsoon convection in Arizona requires careful attention to the evolution of the PBL. Due to the complex terrain, the horizontal and vertical resolution of NWP models is insufficient to resolve all of the important structural details observed in the Arizona PBL and overlying atmosphere. Thus, to produce short-term mesoscale forecasts, forecasters need to conceptually combine features the model can simulate well, such as three-dimensional advective changes, areas of conditional instability, and the basic PBL structure, with their knowledge of the local terrain, local climatology, and features observed in area soundings. Special consideration must be given to features not resolved or predicted by the models, such as the development and advection of many ERLs. The forecaster must attempt to determine (numerically or subjectively) the effect an ERL could have on short-term stability changes, such as its potential to serve as a lid to convective development, and its role in moistening or drying of the PBL.

Verification of four PBL parameterizations in MM5 found that the BLK and MRF schemes more accurately simulate the PBL in terms of temperature, mixing ratio, and depth than the BT and Eta schemes. The BT and Eta schemes, as implemented in MM5, produce PBLs that are too shallow, cool, and moist during the monsoon. It appears the nonlocal schemes' (BLK and MRF) ability to parameterize large eddies affecting the depth of the entire PBL is necessary to simulate properly the deep PBLs that occur over the Southwest. In order to determine the most accurate preconvective PBL forecast, soundings directly contaminated by convection, either modeled or observed, were removed from the study. Nevertheless, it remains possible that our combination of physical parameterizations in MM5 may have contributed to the performance of a particular PBL scheme. In other words, the performance of the Eta or BT PBL schemes may improve if coupled with different physical parameterizations in MM5.

Integrated thermodynamic quantities that are indicative of potential updraft and downdraft strength (CAPE and DCAPE, respectively) also favor the nonlocal BLK and MRF schemes. However, the inhibition of convection (CIN and DTLCL) does not show a significant preference for these schemes. Although the BLK and MRF PBL schemes correctly simulate the development of the afternoon PBL, and to some extent correctly predict the production of CAPE and DCAPE, they do not accurately predict the CIN observed in Southwest soundings. This suggests that the initiation of monsoon convection, rather than the model's ability to forecast areas of conditional instability, may be an important factor that limits the accuracy of MM5 QPFs. Although we arrive at this result through investigation of the MM5 PBL, experiments with the trigger function led Kain and Fritsch (1992) to conclude that, ''. . . the convective trigger function may become the limiting factor in the continued improvement of operational forecasts of mesoscale convective systems.''

To ensure accurate simulation of the monsoon PBL, at least in conjunction with the accompanying model physics tested here, we conclude that deterministic or ensemble MM5 forecasts of the monsoon should use either the BLK or MRF PBL parameterization. (The nonlinearity of the model is such that this result may not apply if the BT or Eta PBL schemes were used in conjunction with different cloud, radiation, or convective parameterizations.) Computationally, the MRF

TABLE 9. As in Table 7 except for DTLCL, the (parcel − environment) temperature at LCL (°C).

Site	Sigma layer	BLK	BT	Eta	MRF	Observed
All	1	−**1.4** (No)	−1.9 (Yes)	−**1.8** (No)	−1.2 (Yes)	−1.6
All	2	−1.3 (Yes)	−2.0 (Yes)	−**1.8** (No)	−1.2 (Yes)	−1.6
All	3	−1.3 (Yes)	−1.9 (Yes)	−**1.8** (No)	−1.1 (Yes)	−1.6
All	4	−1.3 (Yes)	−2.0 (Yes)	−**1.8** (No)	−1.1 (Yes)	−1.7

TABLE 10. Average of the 12-h forecast DCAPE (J kg^{-1}) and its observed value at 0000 UTC for the 21-day period in Aug 1998. The calculations are based on moist descent from the sigma layer just above the LCL. The Yes or No in parentheses indicates whether the difference in the forecast DCAPE from the observed DCAPE is statistically significant at the 5% level. The numbers in bold are the closest to observation.

Site	BLK	BT	Eta	MRF	Observed
ABQ	699 (No)	718 (No)	665 (No)	**662** (No)	637
EPZ	**632** (No)	520 (Yes)	501 (Yes)	543 (No)	704
FGZ	**506** (No)	352 (Yes)	406 (Yes)	468 (No)	547
TUS	869 (No)	662 (Yes)	739 (No)	**811** (No)	783
All	**675** (No)	560 (Yes)	578 (Yes)	621 (No)	665

scheme is 15% faster than BLK, so we typically utilize the MRF PBL parameterization.

It's been shown that short-range ensembles consisting of mixed physical parameterizations result in output that is more dispersive than an ensemble based on a single model configuration (Stensrud et al. 2000). If the ensemble members are weighted equally (Thompson 1977), then a tacit assumption of mixed physics ensembles is that each model configuration is equally likely. Based on the model construction used in our experiments, including the BT or Eta PBL schemes in a mixed physics, monsoon ensemble seems dubious. Nevertheless, because many studies have indicated that the variance of the atmosphere is larger than the variance found in the ensemble (Buizza 1997; Hamill and Colucci 1997, 1998; Stensrud et al. 1999), it may remain tempting (and statistically attractive) to include specific combinations of physical parameterizations to simply increase dispersion without regard to their individual performance. The significant differences between the local and nonlocal schemes tested here raise important questions regarding the construction of mixed ensemble forecast systems. Is improved performance by the ensemble system sufficient reason to include a specific model configuration, known to be inferior and thus not equally likely, in a mixed ensemble? Is it better to exclude that construct from the mix and continue the search for better configurations, such as stochastic model formulations? Or, should the computing resources be used to increase resolution of the superior, equally likely members? It is our belief that improved ensemble performance alone does not constitute sufficient grounds to include a model construct in a mixed ensemble, but that other criteria such as being an equally likely member should also be considered.

The general structure of the PBL predicted by the BLK and MRF schemes, and their predicted CAPE, resembles observations reasonably well. But, their predicted CIN does not. To compensate for this model deficiency, MM5 ensembles that employ variations of the convective trigger function may help account for errors in the model's ability to initiate convection. For this reason, a monsoon ensemble system consisting of initial perturbations, mixed physics, and stochastic processes within the trigger function is the subject of current experiments between the University of Arizona and the NWS office in Tucson.

Acknowledgments. Appreciation is extended to Dr. Robert Maddox for many enlightening discussions on boundary layer processes and convection over Arizona. Dr. David Stensrud (National Severe Storms Laboratory) provided valuable input on MM5 configuration for the monsoon. The reviews of Drs. Jordan Powers (National Center for Atmospheric Research) and David Schultz (National Severe Storms Laboratory) improved both the content and presentation of the manuscript. Three anonymous reviewers improved the manuscript and their input is much appreciated. This work represents a portion of the first author's (DRB) dissertation at the University of Arizona. The second author (SLM) was supported by National Science Foundation Grant ATM-9908968 and Office of Naval Research Grant N00014-99-1-0181. Much of the computational work was supported by Office of Naval Research Grant N00014-00-1-0613.

REFERENCES

Adams, D. K., and A. C. Comrie, 1997: The North American monsoon. *Bull. Amer. Meteor. Soc.*, **78,** 2197–2213.

Anthes, R. A., and T. T. Warner, 1978: Development of hydrodynamical models suitable for air pollution and other mesometeorological studies. *Mon. Wea. Rev.*, **106,** 1045–1078.

——, E.-Y. Hsle, and Y.-H. Kuo, 1987: Description of the Penn State/NCAR Mesoscale Model Version 4 (MM4). NCAR Tech. Note NCAR/TN-282+STR, 66 pp.

Balling, R. C., Jr., and S. W. Brazel, 1987: Diurnal variations in Arizona monsoon precipitation frequencies. *Mon. Wea. Rev.*, **115,** 342–346.

Blackadar, A. K., 1976: Modeling the nocturnal boundary layer. Preprints, *Third Symp. on Atmospheric Turbulence, Diffusion, and Air Quality*, Raleigh, NC, Amer. Meteor. Soc., 46–49.

——, 1978: Modeling pollutant transfer during daytime convection. Preprints, *Fourth Symp. on Atmospheric Turbulence, Diffusion, and Air Quality*, Reno, NV, Amer. Meteor. Soc., 443–447.

Bright, D. R., and D. M. McCollum, 1998: Monitoring Gulf of California moisture surges with *GOES-9* data and the WSR-88D at Yuma, Arizona. Preprints, *16th Conf. on Weather Analysis and Forecasting*, Phoenix, AZ, Amer. Meteor. Soc., 50–52.

Buizza, R., 1997: Potential forecast skill of ensemble prediction and spread and skill distributions of the ECMWF ensemble prediction system. *Mon. Wea. Rev.*, **125,** 99–119.

Burk, S. D., and W. T. Thompson, 1989: A vertically nested regional

numerical weather prediction model with second-order closure physics. *Mon. Wea. Rev.,* **117,** 2305–2324.
Carlson, T. N., R. A. Anthes, M. N. Schwartz, S. G. Benjamin, and D. G. Baldwin, 1980: Analysis and prediction of severe-storms environment. *Bull. Amer. Meteor. Soc.,* **61,** 1018–1032.
——, S. G. Benjamin, G. S. Forbes, and Y.-F. Li, 1983: Elevated mixed layers in the severe-storm environment—Conceptual model and case studies. *Mon. Wea. Rev.,* **111,** 1453–1473.
Chang, J.-T., and P. J. Wetzel, 1991: Effects of spatial variations of soil moisture and vegetation on the evolution of a prestorm environment: A numerical case study. *Mon. Wea. Rev.,* **119,** 1368–1390.
Douglas, M. W., R. A. Maddox, and K. W. Howard, 1993: The Mexican monsoon. *J. Climate,* **6,** 1665–1677.
Dudhia, J., 1989: Numerical study of convection observed during the Winter Monsoon Experiment using a mesoscale two-dimensional model. *J. Atmos. Sci.,* **46,** 3077–3107.
——, 1996: A multi-layer soil temperature model for MM5. Preprints, *Sixth PSU/NCAR Mesoscale Model Users' Workshop,* Boulder, CO, NCAR, 49–50.
Dunn, L. B., and J. D. Horel, 1994a: Prediction of central Arizona convection. Part I: Evaluation of the NGM and Eta Model precipitation forecasts. *Wea. Forecasting,* **9,** 495–507.
——, and ——, 1994b: Prediction of central Arizona convection. Part II: Further examination of the Eta Model forecasts. *Wea. Forecasting,* **9,** 508–521.
Emanuel, K. A., 1994: *Atmospheric Convection.* Oxford University Press, 580 pp.
Farfan, L. M., D. R. Bright, and J. A. Zehnder, 1998: Numerical simulation of mesoscale weather systems in Arizona. Preprints, *12th Conf. on Numerical Weather Prediction,* Phoenix, AZ, Amer. Meteor. Soc., J13–J16.
——, J. A. Zehnder, and D. R. Bright, 2000: Verification of mesoscale model simulations for Arizona. Postprints, *Second Southwest Weather Symp.,* Tucson, AZ, NWS/University of Arizona/COMET, 104–119.
Fritsch, J. M., and J. S. Kain, 1993: Convective parameterization for mesoscale models: The Fritsch–Chappel scheme. *The Representation of Cumulus Convection in Numerical Models, Meteor. Monogr.,* No. 46, Amer. Meteor Soc., 159–164.
Gallus, W. A., Jr., and M. Segal, 2000: Sensitivity of forecast rainfall in a Texas convective system to soil moisture and convective parameterization. *Wea. Forecasting,* **15,** 509–525.
Garratt, J. R., 1992: *The Atmospheric Boundary Layer.* Cambridge University Press, 320 pp.
Giorgi, F., M. R. Marinucci, and G. T. Bates, 1993: Development of a second-generation regional climate model (RegCM2). Part 1: Boundary-layer and radiative transfer processes. *Mon. Wea. Rev.,* **121,** 2794–2813.
Graziano, T. M., and T. N. Carlson, 1987: A statistical evaluation of lid strength on deep convection. *Wea. Forecasting,* **2,** 127–139.
Green, G. D., and J. A. Haro, 1998: Record heat followed by unusually intense dry microbursts and heat bursts over Phoenix on 28 July 1995. Preprints, *16th Conf. on Weather Analysis and Forecasting,* Phoenix, AZ, Amer. Meteor. Soc., 326–328.
Grell, G. A., J. Dudhia, and D. R. Stauffer, 1995: A description of the fifth-generation Penn State/NCAR mesoscale model (MM5). NCAR Tech. Note NCAR/TN-398+STR, 122 pp.
Hales, J. E., Jr., 1975: A severe southwestern desert thunderstorm: 19 August 1973. *Mon. Wea. Rev.,* **103,** 344–351.
Hamill, T. M., and S. J. Colucci, 1997: Verification of the Eta–RSM short-range ensemble forecasts. *Mon. Wea. Rev.,* **125,** 1312–1327.
——, and ——, 1998: Evaluation of the Eta–RSM ensemble probabilistic precipitation forecasts. *Mon. Wea. Rev.,* **126,** 711–724.
Haro, J. A., G. D. Green, and C. L. Dempsey, 1998: Southern Arizona severe convective storms of 14 and 29 August 1996: Similarities and differences. Preprints, *16th Conf. on Weather Analysis and Forecasting,* Phoenix, AZ, Amer. Meteor. Soc., 335–337.
Hoke, J. E., N. A. Phillips, G. J. DiMego, J. J. Tuccillo, and J. G. Sela, 1989: The regional analysis and forecasting system of the National Meteorological Center. *Wea. Forecasting,* **4,** 323–334.
Holtslag, A. A. M., and B. A. Boville, 1993: Local versus non-local boundary layer diffusion in a global climate model. *J. Climate,* **6,** 1825–1842.
Holzworth, G. C., 1964: Estimates of mean monthly maximum mixing depths in the contiguous United States. *Mon. Wea. Rev.,* **92,** 235–242.
Hong, S.-Y., and H.-L. Pan, 1996: Nonlocal boundary layer vertical diffusion in a medium-range forecast model. *Mon. Wea. Rev.,* **124,** 2322–2339.
Janjic, Z. I., 1990: The step-mountain coordinate model: Physical package. *Mon. Wea. Rev.,* **118,** 1429–1443.
——, 1994: The step-mountain Eta coordinate model: Further developments of the convection, viscous sublayer, and turbulence closure schemes. *Mon. Wea. Rev.,* **122,** 927–945.
Johnson, B. C., 1983: The heat burst of 29 May 1976. *Mon. Wea. Rev.,* **111,** 1776–1792.
Kain, J. S., and J. M. Fritsch, 1990: A one-dimensional entraining/detraining plume model and its application in convective parameterization. *J. Atmos. Sci.,* **47,** 2784–2802.
——, and ——, 1992: The role of the convective ''trigger function'' in numerical forecasts of mesoscale convective systems. *Meteor. Atmos. Phys.,* **49,** 93–106.
——, and ——, 1993: Convective parameterization for mesoscale models: The Kain–Fritsch scheme. *The Representation of Cumulus Convection in Numerical Models, Meteor. Monogr.,* No. 46, Amer. Meteor. Soc., 165–170.
Lanicci, J. M., and T. T. Warner, 1991a: A synoptic climatology of the elevated mixed-layer inversion of the southern Great Plains in spring. Part I: Structure, dynamics, and seasonal evolution. *Wea. Forecasting,* **6,** 181–197.
——, and ——, 1991b: A synoptic climatology of the elevated mixed-layer inversion of the southern Great Plains in spring. Part II: The life cycle of the lid. *Wea. Forecasting,* **6,** 198–213.
——, and ——, 1991c: A synoptic climatology of the elevated mixed-layer inversion of the southern Great Plains in spring. Part III: Relationship to severe-storms climatology. *Wea. Forecasting,* **6,** 214–226.
Lieman, R., and P. Alpert, 1993: Investigation of the planetary boundary layer height variations over complex terrain. *Bound.-Layer Meteor.,* **62,** 129–142.
Maddox, R. A., D. M. McCollum, and K. W. Howard, 1993: Case study of an isolated severe thunderstorm over central Arizona: Supercell in the desert? Preprints, *17th Conf. on Severe Local Storms,* St. Louis, MO, Amer. Meteor. Soc., 201–205.
——, ——, and ——, 1995: Large-scale patterns associated with severe summertime thunderstorms over central Arizona. *Wea. Forecasting,* **10,** 763–778.
McCollum, D. M., R. A. Maddox, and K. W. Howard, 1995: Case study of a severe mesoscale convective system in central Arizona. *Wea. Forecasting,* **10,** 641–663.
Mellor, G. L., and T. Yamada, 1974: A hierarchy of turbulence closure models for planetary boundary layers. *J. Atmos. Sci.,* **31,** 1791–1806.
Meltin, J. G., K. W. Howard, and R. A. Maddox, 1991: Southwest area monsoon project. Daily operations summary, 141 pp. [Available from the National Severe Storms Laboratory, 1313 Halley Circle, Norman, OK 73069.]
NCDC, 1995: *Storm Data.* Vol. 37, No. 7, 264 pp. [Available from the National Climatic Data Center, Environmental Data and Information Service, National Oceanic and Atmospheric Administration, Ashville, NC 28801.]
——, 2000: *Storm Data.* Vol. 42, No. 6, 306 pp. [Available from the National Climatic Data Center, Environmental Data and Information Service, National Oceanic and Atmospheric Administration, Ashville, NC 28801.]
Proctor, F. H., 1989: Numerical simulations of an isolated microburst. Part II: Sensitivity experiments. *J. Atmos. Sci.,* **46,** 2143–2165.

Smith, W. P., and R. L. Gall, 1989: Tropical squall lines of the Arizona monsoon. *Mon. Wea. Rev.*, **117,** 1553–1569.

Stackpole, J. D., 1994: The WMO format for the storage of weather product information and the exchange of weather product messages in gridded binary form. NMC/NCEP Office Note 388, 71 pp.

Stensrud, D. J., 1993: Elevated residual layers and their influence on surface boundary-layer evolution. *J. Atmos. Sci.,* **50,** 2284–2293.

——, R. L. Gall, S. L. Mullen, and K. W. Howard, 1995: Model climatology of the Mexican monsoon. *J. Climate,* **8,** 1775–1794.

——, H. E. Brooks, J. Du, M. S. Tracton, and E. Rogers, 1999: Using ensembles for short-range forecasting. *Mon. Wea. Rev.,* **127,** 433–446.

——, J.-W. Bao, and T. T. Warner, 2000: Using initial condition and model physics perturbations in short-range ensemble simulations of mesoscale convective systems. *Mon. Wea. Rev.,* **128,** 2077–2107.

Stull, R. B., 1988: *An Introduction to Boundary Layer Meteorology.* Kluwer Academic Publishers, 670 pp.

Thompson, P. D., 1977: How to improve accuracy by combining independent forecasts. *Mon. Wea. Rev.,* **105,** 228–229.

Wakimoto, R. M., 1985: Forecasting dry microburst activity over the high plains. *Mon. Wea. Rev.*, **113,** 1131–1143.

Watson, A. I., R. E. Lopez, and R. L. Holle, 1994: Diurnal cloud-to-ground lightning patterns in Arizona during the southwest monsoon. *Mon. Wea. Rev.,* **122,** 1716–1725.

Wilks, D. S., 1995: *Statistical Methods in Atmospheric Sciences.* Academic Press, 476 pp.

Wyngaard, J. C., and R. A. Brost, 1984: Top-down and bottom-up diffusion of a scalar in the convective boundary layer. *J. Atmos. Sci.,* **41,** 102–112.

Zhang, D., 1989: The effect of parameterized ice microphysics on the simulation of vortex circulation with a mesoscale hydrostatic model. *Tellus,* **41A,** 132–147.

——, and R. A. Anthes, 1982: A high-resolution model of the planetary boundary layer—Sensitivity tests and comparisons with SESAME-79 data. *J. Appl. Meteor.,* **21,** 1594–1609.

Zipser, E. J., 1977: Mesoscale and convective-scale downdrafts as distinct components of squall-line circulation. *Mon. Wea. Rev.,* **105,** 1568–1589.